diode, and Z_0 is the characteristic impedance of the transmission line in which the diodes are mounted. The average power, P_{AV}, which this same modulator can control, is given by

$$P_{AV} = P_d Z_0 / 2R_s$$

in which P_d is the maximum power each diode can dissipate.

The maximum CW (continuous wave) power P_{max} any 180° phase modulator, using two diodes, can control when mounted in the proper impedance configuration according to Hines [14], is given by

$$P_{max} = E_b[P_d/32R_s]^{1/2}$$

Two diodes having 60-volt breakdown voltage, 4-ohm spreading resistance, and a one-half-watt dissipation rating can control 4.5 watts peak power and about 3 watts average power in a 50-ohm transmission line, or about 4 watts CW power in a 60-ohm transmission line.

The power ratings of diodes switching in the two-path modulator is the same as that of a single-pole, single-throw switch given in Garver [13] and Hines [14].

References

[1] Craig, S. E., W. Fishbein, and O. E. Rittenbach, CW radar with high-range resolution and unambiguous velocity determination, *IRE Trans. on Military Electrics*, vol MIL-6, Apr 1962, pp 153–161.

[2] Montgomery, C. G., *Technique of Microwave Measurements*, M.I.T. Rad. Lab. Ser, vol 11, New York: McGraw-Hill, 1947, p 331.

[3] Rutz, E. M., and J. E. Dye, Frequency translation by phase modulation, *1957 IRE WESCON Conv. Rec.*, pt. 1, pp 201–207.

[4] Rutz, E. M., A stripline frequency translator, *IRE Trans. on Microwave Theory and Techniques*, vol MIT-9, Mar 1961, pp 185–191.

[5] Harmer, J. D., and W. S. O'Hare, Some advances in CW radar techniques, *Proc. 5th Nat'l Conv. on Military Electronics*, Jun 26–28, 1961, pp 311–323.

[6] Stern, E., A variable reactance diode phase shifter, presented at the *1959 PGMTT Nat'l Symposium*, Cambridge: Harvard University.

[7] Hardin, R. H., E. J. Downey, and J. Munushian, Electronically variable phase shifters utilizing variable capacitance diodes, *Proc. IRE*, vol 48, May 1960, pp 944–945.

[8] Searing, R. M., Variable capacitance diodes used as phase shift devices, vol 49, *Proc. IRE*, Mar 1961, pp 640–641.

[9] Dawirs, H. N., and W. G. Swarner, A very fast voltage-controlled, microwave phase shifter, *Microwave J.*, vol 5, Jun 1962, pp 99–107.

[10] White, J. F., Semiconductor microwave phase control, *NEREM Rec.*, 1963, pp 106–107.

[11] Cohen, A. E., Some aspects of microwave phase shifters using varactors, *1962 Proc. 6th Nat'l. Conv. on Military Electronics*, pp 328–332.

[12] White, J. F., High power semiconductor phase shifting devices, Sixth Quart. Prog. Rept. BuShips Cont. NObsr-87291, Microwave Associates, Inc., Burlington, Mass., Apr–Jun 1963.

[13] Garver, R. V., Theory of TEM diode switching, *IRE Trans. on Microwave Theory and Techniques*, vol MTT-9, May 1961, pp 224–238.

[14] Hines, M. E., Fundamental limitations in RF switching and phase shifting using semiconductor diodes, *Proc. IEEE*, vol 52, Jun 1964, pp 697–708.

Circulator Synthesis

JERALD A. WEISS, SENIOR MEMBER, IEEE

Abstract—**A symmetrical three-port ring network composed of reciprocal *T* junctions and nonreciprocal phase shifters is analyzed theoretically to determine conditions under which it exhibits perfect circulation. All physically realizable *T* junctions are considered. It is found that many such junctions, combined with appropriate phase shifters specified by the theory, form perfect circulators. Among these are many cases for which the internal wave amplitudes are small and which require only very small amounts of nonreciprocal phase shift. Circulators designed in accordance with this model may offer appreciable advantages in insertion loss and bandwidth, as well as in mechanical characteristics such as size and weight, and in the possibility of adapting the design for special applications such as high-power capability, high-speed switching, etc. The nature of the model and the method of calculation are summarized.**

Manuscript received August 20, 1964; revised October 12, 1964. This work was performed under the sponsorship of the Array Radars Group of Lincoln Laboratory.

The author is with the Lincoln Laboratory, Massachusetts Institute of Technology, Lexington, Mass. (operated with support from the United States Air Force), and the Worcester Polytechnic Institute, Worcester, Mass.

THEORETICAL CONSIDERATION of the junction circulator has taken the form of group-theoretical treatment of the characteristic modes of symmetrical junctions [1] and analysis of the spatial configurations of the modes [2] under certain simplifying assumptions regarding the structure of the junction. Although a considerable advance in the quality of *Y*-junction circulators has taken place during the same period, it has not been possible to apply the results of the theory to the design effort. The mechanical improvements, which include the shaping of the ferrite, use of composite dielectric-ferrite elements, addition of tuning elements at the ports, and, in strip-line versions, shaping of the center conductor have increased the complexity of the device to the point where simplified theoretical models can serve, at most, only as a qualitative guide.

So long as circulator design remains essentially empirical in nature, there exists the possibility that alternative styles of design offering substantial advantages in one or more specifications may be overlooked. As a familiar example, we may consider the question: how "efficiently" is the volume of ferrite used in present devices? It is now well known that dielectric loading of the junction by the ferrite plays an important part in its performance; designers have found it advantageous, in fact, to replace a considerable fraction of the ferrite by simpler dielectric materials. This naturally leads to speculation as to whether still further improvements might be made if the ferrite and dielectric elements were shaped and distributed in other ways.

As the term synthesis suggests, we attempt to decompose the circulator action into its elementary parts and to specify a combination of these elements which, in a sense, is optimum. If we choose as our optimum, for example, a structure which requires a minimum volume of ferrite, then the object is to characterize the nonreciprocal action separately from the overall scattering by the junction, and to synthesize the structure in such a way that this action is minimized. There is not an obvious reason to suppose in advance that this procedure will lead to results which are of practical significance. We shall show, however, that there do indeed exist circulators which demand only extremely small nonreciprocal effects. Our estimate of losses indicates that there is no penalty in loss in these designs. Estimates of bandwidth are difficult to make without introducing special assumptions regarding the dispersive properties of the components, but there is no indication in the model to be considered that a bandwidth penalty is associated with these designs.

This paper considers a network model in which two aspects of circulator performance are singled out as fundamental: nonreciprocal differential phase shift, regarded as taking place in a distributed manner in the region between the ports; and scattering at the ports, regarded as localized and reciprocal. The relevance of this idealized model to existing circulator designs is based on the observations, 1) that broadband circulation seems to occur only when the electrical distance between ports is at least an appreciable fraction of a wavelength; 2) that coupling to the ports, visualized as localized scattering, must involve internal reflections as a fundamental part of circulator action. No attempt is made here, however, to establish a detailed connection between the network model and a rigorous field theory of junction circulators. Reduction of the complex junction circulator structure to a few disjoint components must, of course, be regarded as a purely conceptual simplification. On the other hand, the model may be regarded as a basis for the synthesis of novel types of circulators. The results of the calculation indicate that some important advantages in performance may be inherent in the ring network to be described.

The ring-network representation of the three-port Y circulator to be considered in this paper is illustrated in Fig. 1, in which the elements L are nonreciprocal phase shifters, and the elements T are symmetrical, reciprocal T junctions. The idea of synthesizing a circulator by joining three ferrite phase shifters has been advanced by others [3], [4], but has not received much attention because it has not appeared to offer any practical advantage over existing junction designs. In the present paper, the network is examined more rigorously. Specifically, the role of reflections at the T junctions in determining the characteristics of the circulator is incorporated in a systematic way.

The most significant result of the theory is the discovery that the ring network may exhibit perfect circulation even when the amount of phase differential for propagation around the ring in the two-clock senses is very small. This result by itself is not unexpected: a familiar circulator theorem asserts that *any* nonreciprocal three-port junction can be made to circulate by the addition of obstacles at the ports. It is found, however, that the amplitudes of the standing waves excited within the ring are surprisingly small in many cases. Some examples are presented in Tables I and II. As will be explained in the subsequent discussion and appendices, the example of Table I requires nonreciprocal phase shifters having a differential phase of only about 8° per sector; yet, the amplitude of the standing waves in the sectors adjoining the isolated port is only a little over twice the amplitude of the incident signal. A measure of merit of such a circulator may be formulated in terms of the amount of nonreciprocal phase and the amplitudes of the internal standing waves. This quantity turns out to be quite insensitive to the amount of nonreciprocal phase and, in fact, slightly lower (corresponding to lower insertion loss) in many of the low-phase cases than in those of higher phase. This means that in the designs prescribed by the theory for which the required differential phase is small, the saving in insertion loss due to the requirement of only a small volume of nonreciprocal medium (ferrite), more than compensates for the penalty in insertion loss resulting from the relatively large amplitudes of the interval waves.

The theory also yields a prescription for the frequency dependence of the scattering at the T's, such that circulation may be made to persist over a band of any width (with, of course, increasing complexity of structure as the bandwidth specification is increased). Thus, if the frequency dependence of the intrinsic reciprocal and nonreciprocal phases of the ferrite-loaded junction is known, the characteristics of the corresponding T junctions required for circulation over the entire band are completely determined. For the types of differential phase shifter characteristics commonly encountered in waveguide and coaxial device practice, it is reasonable to expect that the required T's can be synthesized by the application of known filter principles, resulting in a rigorously flat broadband Y-junction circulator, which exhibits only incidental loss and which may be built with extremely efficient use of ferrite. Depending on the

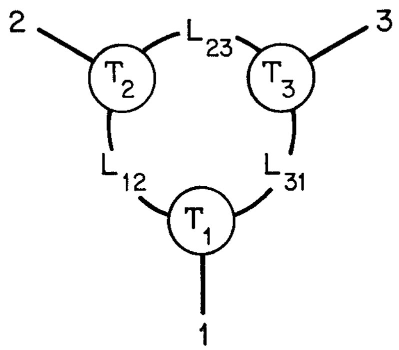

Fig. 1. The ring network. T and L denote symmetrical T junctions and nonreciprocal phase shifters, respectively.

TABLE I

THE RING-NETWORK CIRCULATOR, CASE (27°; 631B)

	Magnitude	Phase, degrees
r	0.254	170.17
s	0.878	58.68
r_d	0.820	14.55
s_d	0.405	135.00
ϵ	1.00	58.12
δ	1.00	3.97
ϕ_+	—	62.09
ϕ_-	—	54.15
$\Delta\phi$	—	7.94
E_1	0	—
E_2	1.00	9.69
E_3	0	—
C_{12}	1.56	153.82
C_{23}	1.12	−79.71
C_{31}	1.12	27.38
D_{21}	1.20	22.25
D_{32}	1.12	−152.69
D_{13}	1.12	108.16
M	4.94	—

TABLE II

THE RING-NETWORK CIRCULATOR

Summary of ten cases, identified as (γ; 631b) with $\gamma=4.50°, \cdots, 45.00°$. Listed with γ are the nonreciprocal phase parameter arg δ, the amplitude of the internal wave C_{31}, and the parameter of merit $M=|C_{31}|^2$ arg δ. The magnitudes of the scattering coefficients of the T junctions are also listed. Additional details of the case $\gamma=27°$ are given in Table I.

γ	4.50	9.00	13.50	18.00	22.50	27.00	31.50	36.00	40.50	45.00
arg δ	0.137	0.539	1.18	2.02	2.98	3.97	4.88	5.56	5.91	5.85
$\|C_{31}\|$	5.92	2.98	2.02	1.55	1.28	1.12	1.02	0.962	0.948	0.971
M	4.79	4.80	4.81	4.84	4.88	4.94	5.03	5.15	5.31	5.52
$\|r\|$	0.379	0.367	0 347	0.321	0.290	0.254	0.217	0.183	0.156	0.146
$\|s\|$	0.922	0.917	0.910	0.900	0.889	0.878	0.869	0.861	0.855	0.854
$\|r_d\|$	0.994	0.976	0.947	0.910	0.866	0.820	0.777	0.740	0.716	0.707
$\|s_d\|$	0.078	0.155	0.227	0.294	0.354	0.405	0.446	0.476	0.494	0.500

application contemplated, this efficiency may be manifested in some combination of compact size, low-loss, high-peak and average-power capacity, high-speed reversal of the direction of circulation, etc.

The method of carrying out the network analysis is as follows. The scattering coefficients of a symmetrical T junction are expressed in terms of the characteristic modes of the junction. The derivation follows the standard method [5] of the theory of group representations, but the result is obtained with full generality not found in standard treatments of the subject so as to represent all physically realizable T junctions satisfying reciprocity, energy conservation, and T symmetry. The scattering of a matched, lossless, nonreciprocal phase shifter (denoted by L in Fig. 1) is represented by a reciprocal, or average, phase factor $\epsilon=\exp\, i(\phi_+ + \phi_-)/2$, and a nonreciprocal, or differential phase factor $\delta=\exp\, i(\phi_+ - \phi_-)/2$, where ϕ_+ and ϕ_- refer to clockwise and counterclockwise propagation, respectively. The overall scattering by the network is then calculated in terms of the parameters of the T's and L's. We obtain the scattering coefficients E_1, E_2, and E_3 denoting, respectively, reflection, transmission, and leakage in response to a unit signal incident on port 1 of the ring.

The conditions for perfect circulation are now imposed on the overall scattering coefficients E_1, E_2, E_3. They are: input match, $E_1=0$; perfect isolation, $E_3=0$; lossless transmission, $|E_2|=1$. These conditions are, of course, not mutually independent; on the contrary, the last condition implies the other two. It turns out to be convenient, however, to use the isolation condition $E_3=0$; solving this relation to find the reciprocal phase factor ϵ and the nonreciprocal phase factor δ, we obtain a biquartic, algebraic equation for ϵ and an expression for δ in terms of ϵ, both relations involving the scattering coefficients of the T's as parameters. The problem now becomes one of computation.

A program was written for the MIT Lincoln Laboratory IBM 7094-C computer, in which values were assigned to the scattering coefficients of the T's in sets (cases) covering the range of physically realizable T's in a convenient number of steps. For each case, the problem was solved to find (a) the phase factors ϵ and δ if they exist; (b) the amplitudes and phases of the internal waves excited by a unit wave incident on port 1 of the ring; (c) the phase of the transmitted wave E_2; (d) the

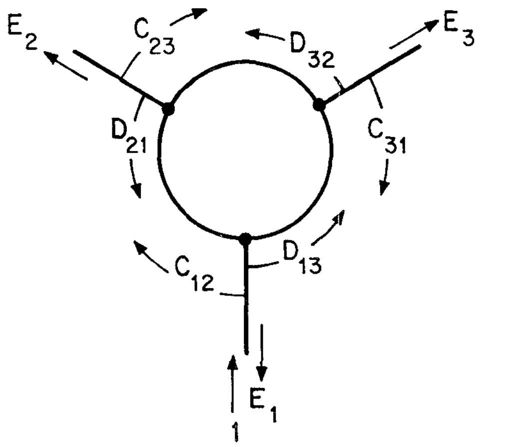

Fig. 2. Internal and scattered waves in the ring network.

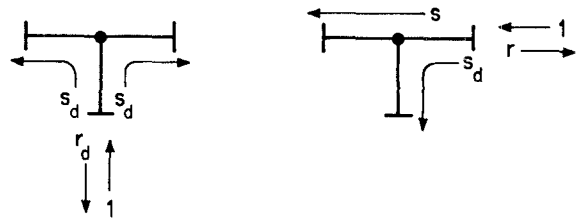

$$S_T = \begin{bmatrix} r & s & s_d \\ s & r & s_d \\ s_d & s_d & r_d \end{bmatrix}$$

Fig. 3. Definition of the scattering matrix of a symmetrical T junction.

quantity M, defined subsequently, which provides an estimate of the relative insertion loss. In all, about 700 cases were considered. Of these, well over half gave solutions satisfying all requirements. As an example, the case identified as (27°; 631b) is summarized in Table I. The scattering coefficients r, s, r_d, and s_d of the T's are defined in Fig. 3, and the internal partial waves C and D are defined in Fig. 2.

The table first lists the four scattering coefficients of the T junctions. They specify what would ordinarily be considered "poorly" matched junctions; for example, the coefficient r_d specifying reflection at the accessible port d (Fig. 3) has the magnitude 0.820 corresponding to a VSWR (voltage standing-wave ratio) of 10/1 for the T junction if its other ports were terminated in matched loads. When combined to form the ring, these T's, together with the corresponding L's yield, of course, a perfectly matched circulator.

The next series of entries specifies the characteristics of the phase shifters. The most significant number is the parameter δ which defines the differential phase $\Delta\phi$ through the relation $\Delta\phi = 2 \arg \delta$. In this example, $\Delta\phi$ is only 7.94° (per sector). The parameter ϵ specifying the average phase per sector is of less significance, since it can be "traded" with the phases of the scattering coefficients of the T's without affecting δ or the amplitudes of the internal waves.

The overall scattering coefficients E_1, E_2, and E_3 are listed next. They verify that perfect circulation indeed does occur and specify, through the phase of E_2, the overall phase of transmission through the ring.

The amplitudes of the C's and D's, the six internal wave amplitudes (Fig. 2) are listed. The total standing-wave amplitudes in the sectors 2–3 and 3–1 are the sums $C_{23}+D_{32}$ and $C_{31}+D_{13}$, respectively. In this example, they are equal to 2.24 times the amplitude of the signal incident on port 1.

A measure of the merit of the network with respect to its dissipative losses may be obtained from these data, notwithstanding the fact that dissipative effects have been neglected in the model. We make the plausible assumption that the dominating contribution to loss is magnetic in origin, and take the loss, as characterized by the Poynting theorem, to be proportional to the product of $\arg \delta$ (which measures the required length of the differential phase shifters) times $|C_{31}|^2$ (which measures the power level of the internal standing-wave configuration). The value of this product M for the present example is $M = 4.94$. The significance of this value of M may be seen when the case presented in Table I is compared with others in a series, as shown in Table II.

Table II lists a series of ten cases, showing values of $\arg \delta$ ranging from less than one degree to about 6°, with a corresponding decrease in $|C_{31}|$ from about six to about one. A number of details of the solutions have been omitted in order to emphasize the most significant features. The competition between $\arg \delta$ and $|C_{31}|$ results in a value of the parameter M which remains quite stable but shows a slight increase as $\arg \delta$ increases. This suggests that the very small-phase ring circulator designs are actually of higher merit (lower M) as far as magnetic losses are concerned, although other sources of loss might overbalance this tendency when the wave amplitudes become large.

In Appendices I and II, some further details are presented relating to the evaluation of the scattering matrix of the T junction, and the solution of the ring network problem.

Appendix I

The Scattering Matrix of a Symmetrical T Junction

The logic of the ring-circulator theory, whereby we begin with an assumed scattering matrix S_T for the three T junctions and calculate the corresponding requirements on the nonreciprocal phase shifters, demands that we have a completely general formulation of S_T, such that all physically realizable T junctions are represented. Since this is more general than that found in the standard treatments of the problem, we summarize here the derivation of S_T.

The T junctions are characterized by T symmetry, reciprocity, and losslessness. Reciprocity and energy conservation are represented, respectively, by symmetry and unitarity of the scattering matrix

$$\tilde{S}_T = S_T$$
$$S_T^\dagger S_T = I$$

where $\sim$ denotes the transpose, $\dagger$ the Hermitean conjugate, and I the unit matrix. T symmetry is represented by invariance of S_T with respect to a reflection which interchanges the two symmetrical ports of the junction. Let P denote the reflection operator represented by the matrix

$$P = \begin{bmatrix} 0 & 1 & 0 \\ 1 & 0 & 0 \\ 0 & 0 & 1 \end{bmatrix}$$

Then

$$P^{-1} S_T P = S_T$$

or

$$S_T P - P S_T = 0$$

that is, S_T commutes with P. Since the two matrices commute, there exists a unitary transformation matrix M which simultaneously diagonalizes S_T and P. We find M by carrying out the diagonalization of the reflection matrix P. The result is

$$M^\dagger P M = \begin{bmatrix} -1 & 0 & 0 \\ 0 & +1 & 0 \\ 0 & 0 & +1 \end{bmatrix}$$

where

$$M = \frac{1}{\sqrt{2}} \begin{bmatrix} 1 & e^{i\phi_b} \cos\gamma & e^{i\phi_c} \sin\gamma \\ -1 & e^{i\phi_b} \cos\gamma & e^{i\phi_c} \sin\gamma \\ 0 & \sqrt{2}\, e^{i\phi_b} \sin\gamma & -\sqrt{2}\, e^{i\phi_c} \cos\gamma \end{bmatrix}$$

in which ϕ_b, ϕ_c, and γ are arbitrary real angles. The dependence of M on γ is a consequence of the degeneracy in the eigenvalues of P. We may assume, for the diagonal representation of S_T, the form

$$M^\dagger S_T M = \begin{bmatrix} s_a & 0 & 0 \\ 0 & s_b & 0 \\ 0 & 0 & s_c \end{bmatrix}$$

where s_a, s_b, and s_c are complex numbers of unit magnitude but otherwise arbitrary. Reversing this transformation, we obtain

$$S_T = \begin{bmatrix} r & s & s_d \\ s & r & s_d \\ s_d & s_d & r_d \end{bmatrix}$$

where

$$r = \tfrac{1}{2}(s_a + s_b \cos^2\gamma + s_c \sin^2\gamma)$$
$$s = \tfrac{1}{2}(-s_a + s_b \cos^2\gamma + s_c \sin^2\gamma)$$
$$r_d = s_b \sin^2\gamma + s_c \cos^2\gamma$$
$$s_d = \frac{1}{\sqrt{2}}(s_b - s_c)\cos\gamma \sin\gamma$$

All T junctions satisfying T symmetry, reciprocity, and energy conservation are characterized by this set of scattering coefficients. For computing purposes, we express s_a as exp $(i\sigma_a)$, and similarly for s_b and s_c. We assign values of σ_a and σ_b in the range $0 \leq \sigma_a, \sigma_b < 2\pi$; σ_c can be held fixed at zero without loss of generality. We assign values of γ in the range $0 < \gamma \leq \pi/4$.

Appendix II

The Ring Circulator Problem

With the scattering coefficients of the T junctions (Fig. 3) characterized as discussed in Appendix I, we may analyze the scattering within the ring network (Fig. 2) as follows: the scattered wave C_{12}, for example, is composed of contributions due to transmission of the unit incident signal into the sector 1–2, the transmission of the wave C_{31} from sector 3–1 into sector 1–2, and the reflection of D_{21} at the T junction and we get

$$C_{12} = s_d + sC_{31}e^{-i\phi_+} + rD_{21}e^{-i\phi_-} \tag{1}$$

Let

$$e^{-\frac{1}{2}i(\phi_+ + \phi_-)} = \epsilon \tag{2}$$
$$e^{-\frac{1}{2}i(\phi_+ - \phi_-)} = \delta \tag{3}$$
$$r\epsilon = R \tag{4}$$
$$s\epsilon = S \tag{5}$$

Using (2), $\cdots$, (5) in (1), we have

$$C_{12} = s_d + \delta S C_{31} + \delta^* R D_{21} \tag{6}$$

Figure 4 illustrates schematically the composition of (6). Similarly, we may construct six relations connecting the C's and D's. In matrix form they are

$$\begin{bmatrix} \delta^* R & -1 & & & & \delta S \\ -1 & \delta R & \delta^* S & & & \\ & \delta S & \delta^* R & -1 & & \\ & & -1 & \delta R & \delta^* S & \\ & & & \delta S & \delta^* R & -1 \\ \delta^* S & & & & -1 & \delta R \end{bmatrix} \begin{bmatrix} D_{21} \\ C_{12} \\ D_{32} \\ C_{23} \\ D_{13} \\ C_{31} \end{bmatrix} = -s_d \begin{bmatrix} 1 \\ \\ \\ \\ \\ 1 \end{bmatrix} \tag{7}$$

In (7), null elements have been omitted for clarity. Expressions for the waves E_1, E_2, and E_3 scattered out of the ring at the three ports may be formed in the same way. We obtain

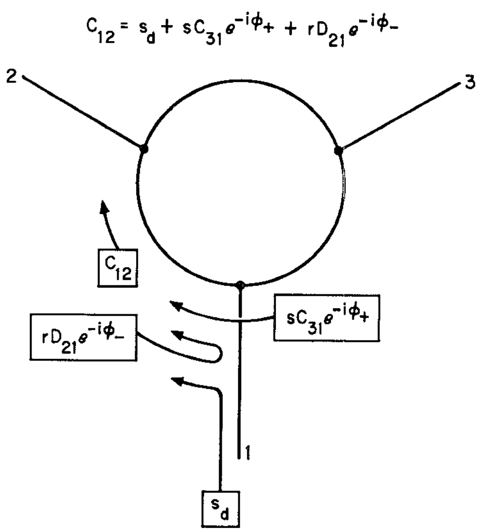

Fig. 4. Illustrating the composition of the scattering equations for the ring network.

$$E_1 = r_d + \epsilon s_d(\delta C_{31} + \delta^* D_{21}) \tag{8}$$

$$E_2 = \epsilon s_d(\delta C_{12} + \delta^* D_{32}) \tag{9}$$

$$E_3 = \epsilon s_d(\delta C_{23} + \delta^* D_{13}) \tag{10}$$

Solving the system (7), we obtain for the C's,

$$C_{12} = -\frac{s_d}{\Delta}\{[R(R-S)(R^2-S^2-1)+(1-R^2)] + \delta^{*3}S^2(R-S)\} \tag{11}$$

$$C_{23} = -\frac{s_d}{\Delta}\{\delta^{*2}S[R-(R-S)^2(R+S)] - \delta S(R^2-RS-1)\} \tag{12}$$

$$C_{31} = -\frac{s_d}{\Delta}\{\delta^*[(R-S)^3(R+S)^2 - R(2R^2-RS-S^2-1)] + \delta^2 S^2\} \tag{13}$$

where

$$\Delta = (R^2-S^2)^3 - 3R^2(R^2-S^2-1) + (\delta^3+\delta^{*3})S^3 - 1 \tag{14}$$

The D's may be found similarly by direct calculation, but we note that they are related to the C's in a simple way as a consequence of the symmetry of the network, as manifested in the form of the system (7). Under interchange of δ and δ^*, that is, $\delta \leftrightarrow \delta^*$, the C's and D's are interchanged according to

$$C_{12} \leftrightarrow D_{13}$$
$$C_{23} \leftrightarrow D_{32}$$
$$C_{31} \leftrightarrow D_{21}$$

Now, using the C's and D's in (8), (9), and (10), we obtain the desired expressions for the scattered waves

$$E_1 = r_d - \epsilon\frac{s_d^2}{\Delta}\{2(R-S)[(R^2-S^2)^2 - R(2R+S)] + (\delta^3+\delta^{*3})S^2 + 2R\} \tag{15}$$

$$E_2 = -\delta\epsilon\frac{s_d^2}{\Delta}\{(R-S)^3(R+S) - 2R(R-S) + \delta^{*3}S[1-(R-S)^2] + 1\} \tag{16}$$

$$E_3 \leftrightarrow E_2 \qquad \text{under} \qquad \delta \leftrightarrow \delta^* \tag{17}$$

We now impose a requirement for perfect circulation,

$$E_3 = 0 \tag{18}$$

describing perfect isolation of port 3. For a lossless three-port junction, this condition implies either perfect circulation, $|E_2| = 1$, or complete reflection at the input, $|E_1| = 1$. We discard the latter solutions. With E_3 given by (17), (18) yields

$$0 = (R-S)^3(R+S) - 2R(R-S) + \delta^3 S[1-(R-S)^2] + 1 \tag{19}$$

Using (4) and (5), we obtain from (19)

$$(a_4\epsilon^4 + a_2\epsilon^2 + a_0) + (a_3\epsilon^3 + a_1\epsilon)\delta^3 = 0 \tag{20}$$

where

$$\left.\begin{aligned} a_4 &= (r-s)^3(r+s) \\ a_3 &= -s(r-s)^2 \\ a_2 &= -2r(r-s) \\ a_1 &= s \\ a_0 &= 1 \end{aligned}\right\} \tag{21}$$

Solving (20) for δ in terms of ϵ, we have

$$\delta^3 = -\frac{a_4\epsilon^4 + a_2\epsilon^2 + a_0}{a_3\epsilon^3 + a_1\epsilon} \tag{22}$$

With the requirements from (2) and (3) that

$$|\delta| = |\epsilon| = 1 \tag{23}$$

we obtain from (22) the following biquartic equation in ϵ:

$$A_8\epsilon^8 + A_6\epsilon^6 + A_4\epsilon^4 + A_2\epsilon^2 + A_0 = 0 \tag{24}$$

where

$$\left.\begin{aligned} A_8 &= A_0^* = a_4 a_0^* \\ A_6 &= A_2^* = a_4 a_2^* + a_2 a_0^* - a_3 a_1^* \\ A_4 &= |a_4|^2 + |a_2|^2 + |a_0|^2 - |a_3|^2 - |a_1|^2 \end{aligned}\right\} \tag{25}$$

Equation (24) is the basis for the numerical solution of the problem. To solve a single case we select a set of values for the angles σ_a, σ_b, σ_c, and γ characterizing the scattering matrix S_T as discussed in Appendix I. Using these, we compute and record the four scattering coefficients r, s, r_d, and s_d of the T junctions. In terms of the coefficients r and s, we successively evaluate the coefficients $a_0, \cdots, a_4$, (21), and the coefficients $A_0, \cdots, A_8$, (25). We then solve (24) for ϵ and use (22) to evaluate δ. We test to ascertain that the magnitudes of ϵ and δ fulfill the requirement (23); if they do, the case yields a physically realizable circulator. We proceed to evaluate the C's and D's specified by (11), (12), and (13), and the

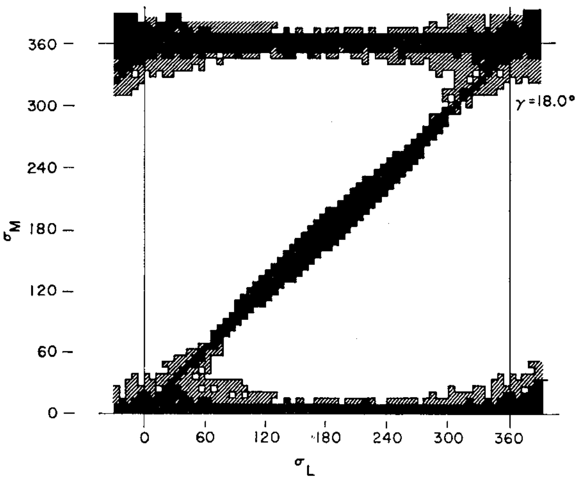

Fig. 5. A map of the σ_L, σ_M plane for $\gamma=18.0°$.
White: physically realizable ring circulators;
Black: no ring circulator exists;
Shaded: borderline cases, uncertain due to rounding-off errors.

overall transmission coefficient E_2, (9). Finally, the parameter of merit M is evaluated.

A map illustrating the range of soluble cases is shown in Fig. 5. The particular range of cases shown there is for the value $\gamma=18.0°$ and $\sigma_c=0$, with σ_a and σ_b ranging from 0° to 360° (σ_L and σ_M are the same as σ_a and σ_b, respectively). The white areas represent physically realizable cases; the black, inadmissible cases. The diagonally shaded regions are borderline cases which are ambiguous because of rounding-off errors in the computation. A series of eleven such maps, for $\gamma=0°$, 4.5°, · · · , 45.0°, show that well over half of the "parameter space," whose coordinates are σ_a, σ_b, σ_c, γ, is occupied by physically realizable cases.

Acknowledgment

The support and encouragement of D. H. Temme and other members of the group is hereby acknowledged. I also wish to acknowledge the invaluable assistance of J. Tabasky and C. Work of the Computer Facility of the Lincoln Laboratory.

References

[1] Auld, B. A., The synthesis of symmetrical waveguide circulators, *IRE Trans. on Microwave Theory and Techniques*, vol MTT-7, Apr 1959, pp 238–246.
[2] Bosma, H., On the principle of stripline circulation, *Proc. IEE* (London), vol 109B, suppl 21, 1962, p 137.
——, On stripline Y-circulation at UHF, *IEEE Trans. on Microwave Theory and Techniques*, vol MTT-12, Jan 1964, pp 61–72.
[3] Grace, M., and F. R. Arams, Three-port ring circulators, *Proc. IRE* (*Correspondence*), vol 48, Aug 1960, p 1497.
[4] Vartanian, P. N., The theory and applications of ferrites at microwave frequencies, Sylvania EDL Rept. DDC-101, 888, Sylvania Defense Lab., Mountain View, Calif., Apr 1956.
[5] Montgomery, C. G., R. H. Dicke, and E. M. Purcell, *Principles of Microwave Circuits*, M.I.T. Rad. Lab. Ser., vol 8, ch. 12, New York: McGraw-Hill, 1948.

A 7-Gc/s Narrow-Band Waveguide Switch Using *p-i-n* Junction Diodes

H. J. PEPPIATT, MEMBER, IEEE, A. V. McDANIEL, JR., AND J. B. LINKER, JR., SENIOR MEMBER, IEEE

***Abstract*—A narrow-band waveguide switch with power capability in excess of 8 watts has been designed in WR137 waveguide. *p-i-n* diodes are used in band elimination filter sections. The attenuation in the reject band is greater than 80 dB over a 10 Mc/s range, and the passband loss is less than 0.5 dB.**

Introduction

IN BOTH the forward and reverse bias conditions, the *p-i-n* diode approximates very closely a linear circuit element. Hence, conventional circuit analysis and synthesis can be used in the design of components using these diodes. The microwave switch, to be described here, can be designed by the use of waveguide band elimination filter synthesis.

Manuscript received June 15, 1964; revised October 19, 1964.
The authors are with the Communication Products Dept., General Electric Co., Lynchburg, Va.

Band Elimination Synthesis

For completeness, a very brief resume of a band elimination synthesis is included. The low-pass prototype of Fig. 1 can be synthesized to a given response by modern network techniques. Extensive tables giving the element values for a wide variety of responses are available.[1] The frequency and impedance transformations necessary to arrive at a quarter-wave coupled band elimination filter are shown in Fig. 1. It is easily shown that

$$y_p'' = -jY_0 g_p \frac{\omega_b}{\omega_0 \Omega} \tag{1}$$

[1] Weinberg, L., *Network Analysis and Synthesis*, New York: McGraw-Hill 1962, pp 604–631.